

Semi-empirical Calculations for the Second Hyperpolarizabilities of Pyrrole and Furan Oligomers

Won-Hyung Kim

Department of Chemistry, College of Natural Sciences, Cheju National University

Pyrrrole과 Furan Oligomer의 2차초편극도에 대한 반경험적 계산 연구

김 원 형

제주대학교 자연과학대학 화학과

Abstract

All-trans geometries of pyrrole and furan oligomers have been fully optimized and their second hyperpolarizabilities have been calculated using AM1, MNDO, and PM3 semi-empirical approximations by means of finite-field method. The large γ values were obtained with fully extended π electron delocalization system. The increase of γ is linearly dependent on the conjugatin length of the oligomers. Predicted limiting γ values per subunit were calculated using $/n$ and $/s$ methods, and $/s$ converged to the asymptotic values faster than $/n$ at moderate oligomer sizes. The $/s$ limiting γ values were twice the $/n$ values up to 9 rings of the oligomers considered here, however the same result should be given at the infinite polymer limit.

Introduction

Since the advent of lasers in 1960s, the study of nonlinear optical properties in various materials has been accelerated and its applications have been made into a variety range

of optoelectronics¹⁻³. Recently the search for the materials showing high NLO properties is concentrated theoretically as well as experimentally⁴, but the experimental data have not yet been collected with quite satisfactory amounts so far. For the viewpoint of

computations, on the other hand, the predictions and discussions about NLO properties of many organic compound candidates have been possible due to the tremendous development of computational capabilities in software as well as hardware terms for scientific environment.

The nonlinear optical property here is meant by the nonlinear behavior of the polarization of a molecule when it is exposed to a high external electric field. For being a good candidate as materials having highly nonlinear optical responses, it is well known to possess highly acentrosymmetric systems for the first hyperpolarizabilities (β) and highly delocalized π electron systems for the second hyperpolarizabilities (γ), where the first and second hyperpolarizabilities are the nonlinear optical responses of materials^{2,3}. The first and second hyperpolarizabilities are directly related with the second harmonic generation and the third harmonic generation in nonlinear optics, respectively.

Heterocyclic organic compounds are well known to exhibit significant NLO behavior, and it is of importance to investigate the second hyperpolarizabilities of such systems with respect to the increase of the chain length. In this study, the second hyperpolarizabilities for the oligomers of pyrrole and furan with up to 9 heterocyclic rings were calculated in three different semi-empirical molecular orbital approximations (AM1, MNDO,

and PM3 methods), and their behaviors on increasing the repeating units were investigated to predict the NLO properties for larger polymer systems. The second hyperpolarizability values reported here are the calculated ones with a static electric field using the finite-field method⁵ so that there may exist some problems to directly compare with the experimental results if available, due to various experimental factors as well as the frequency dependent nature.

Computational Methods

The polarization, P , induced in a medium by an external electric field E is usually given by

$$P = P^0 + \chi^{(1)} \cdot E + \chi^{(2)} \cdot E \cdot E + \chi^{(3)} \cdot E \cdot E \cdot E + \dots$$

where $\chi^{(n)}$ are the n -th order susceptibility tensors of the bulk medium. The nonlinear optical properties of materials arise from nonzero values of the terms higher than $\chi^{(1)}$. These bulk susceptibilities can be expressed in terms of the molecular induced dipole moment which is related to the molecular polarizability and hyperpolarizability tensors with the applied electric field as a power series, and it can be written as⁶

$$\mu_i = \mu_i^0 + \alpha_{ij} E_j + (1/2!) \beta_{ijk} E_j E_k + (1/3!) \gamma_{ijkl} E_j E_k E_l + \dots$$

where μ_i^0 is the i component of the permanent dipole moment of a substance and α_{ij} , β_{ijk} , and γ_{ijkl} are the tensor elements of the polarizability, the first hyperpolarizability, and the second hyperpolarizability, respectively. In the above expression, E_j is the j component of the applied electric field acting on the molecule, and the subscripts are the Cartesian coordinates. The energy W of the molecule also can be related to its dipole moment μ in an external electric field E using the relationship of $W = -\int \mu dE$ such as

$$\begin{aligned} W = & W^0 - \mu_i^0 E_i - (1/2!) \alpha_{ij} E_i E_j \\ & - (1/3!) \beta_{ijk} E_i E_j E_k \\ & - (1/4!) \gamma_{ijkl} E_i E_j E_k E_l \\ & - \dots \end{aligned}$$

where W^0 is the energy of the molecule in the absence of the external electric field. The α_{ij} , β_{ijk} , and γ_{ijkl} are all polar tensors fully symmetric in the permutation of the Cartesian indices, and allow the induced dipole moment to be in a direction other than that of the applied electric field. The coefficients are obtained by finite differencing successively at static field ($E_i = 0$) such as

$$\begin{aligned} \mu_i^0 &= -\left(\frac{\partial W}{\partial E_i}\right) \\ \alpha_{ij} &= -\left(\frac{\partial^2 W}{\partial E_i \partial E_j}\right) \\ \beta_{ijk} &= -\left(\frac{\partial^3 W}{\partial E_i \partial E_j \partial E_k}\right) \\ \gamma_{ijkl} &= -\left(\frac{\partial^4 W}{\partial E_i \partial E_j \partial E_k \partial E_l}\right) \end{aligned}$$

In the finite-field method, the perturbed hamiltonian for the molecule can be written as⁷

$$H' = H - \sum_i E r_i$$

where E is a finite electric field, and r_i is the position operator for the i -th electron. From the variational Hartree-Fock procedure, this perturbation term results in a modified form for the standard Hartree-Fock matrix elements as

$$F_{\lambda\nu} = F_{\lambda\nu}^0 + \sum_i E_i D_{\lambda\nu}^i$$

where $F_{\lambda\nu}^0$ is the unperturbed zero field Hartree-Fock matrix element and

$D_{\lambda\nu}^i$ is the i -th component of the dipole moment matrix element between atomic orbitals ϕ_λ and ϕ_ν . In the semi-empirical MO approximations used here, $D_{\lambda\nu}^i$ is neglected unless ϕ_λ and ϕ_ν are atomic orbitals on the same atom. From the resulting perturbed wavefunctions, all the tensor components including the hyperpolarizabilities are obtained by successively computing $W(E)$ for a series of positive and negative electric field strengths of the same magnitude.

In order to get the orientationally averaged values, the mean values for the polarizability and hyperpolarizability tensors are necessary such as⁶,

$$\langle a \rangle = \frac{1}{3} (a_{xx} + a_{yy} + a_{zz})$$

$$\langle \beta \rangle = \frac{3}{5}(\beta_{ixx} + \beta_{iyy} + \beta_{izz})$$

$$\langle \gamma \rangle = \frac{1}{5}(\gamma_{xxxx} + \gamma_{yyyy} + \gamma_{zzzz} + 2\gamma_{xxyy} + 2\gamma_{yyzz} + 2\gamma_{zzxx})$$

where x , y , z denote Cartesian components, and i is the major symmetry axis that coincides with the dipole moment vector. The second hyperpolarizabilities of the pyrrole and furan oligomers reported in this paper are therefore the average values of $\langle \gamma \rangle$.

For the calculation of the second hyperpolarizabilities in the finite-field method, the applied electric field strength should be chosen properly. It must be high enough to show the nonlinear optical responses from a molecule, but not exceed to the limit over which the molecular electronic structure distortion would occur. Also, too high electric field strength may cause the terms following after the γ terms in the above power series expressions to be significant so that they would not be truncated in the finite-field method. The electric field strength adopted in this work was 0.001 a.u. which is equivalent to 5.1423×10^6 V/cm, and this choice was shown quite reasonable⁸.

The finite-field procedure has been modified in MOPAC program⁹, which allows the calculation of nonlinear optical properties as well as geometry optimization of a molecule on each AM1, MNDO, and PM3 hamiltonians¹⁰. The oligomers of pyrrole and furan studied in this paper were fully optimized in all-trans forms with three semi-empirical levels and then taken to the second hyperpolarizability calculations. The all-trans geometries of these oligomers are shown in Figure 1.

The atomic unit (a.u.) was used in this paper for the unit of the second hyperpolarizability, where one a.u. of γ equals to 5.0509×10^{-40} esu, which is equivalent to 6.2356×10^{-65} C⁴m⁴J⁻³.

Results and Discussion

In order to achieve the best nonlinear optical behaviors, the geometry optimization procedure was fully performed for the all-trans polypyrroles and polyfurans. For the all-trans pyrrole oligomers, the stable geometries were obtained from a dimer size up to the oligomer with nine pyrrole rings using AM1, MNDO and PM3 methods, and their heats of

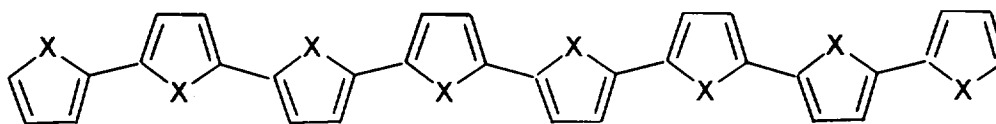


Figure 1. Structure of the all-trans eight-ring pyrrole(X=NH) and furan(X=O) oligomers

formation are shown in Figure 2. The values increase quite constantly with the increase of the number of pyrrole rings, but the AM1 results are the highest among the three different methods. These oligomer structures were confirmed as a trans conformation in which the dihedral angles between two adjacent pyrrole rings were observed to be almost exactly 180° from the geometry optimization result by AM1 and PM3 methods. However, from the results of MNDO method, the optimized geometry of the pyrrole oligomers that were initially proposed as a perfectly trans structure in the beginning of the calculation showed a distorted, twisted conformation in which the dihedral angles between two adjacent rings were about 114° . Therefore the MNDO optimized geometries and so those heats of formation shown here are not for the true all-trans pyrrole oligomer structures. The same procedure has been done for the all-trans furan oligomers up to eight furan rings, and their heats of formation are shown in Figure 3. In this case, all three semi-empirical methods gave fully optimized conformations of all-trans furan oligomers in which the dihedral angles between two adjacent furan rings were almost 180° . The AM1 heats of formation increase with the increase of the number of furan rings, however those from PM3 were almost not changed, and those from MNDO decreased with a constant rate. The

discrepancy between them is due to the different parameterizations of three molecular orbital approximations.

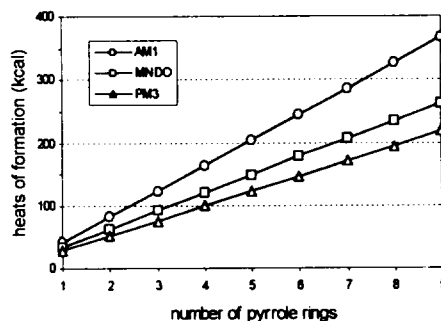


Figure 2. Heats of formation in kcal for all-trans pyrrole oligomers

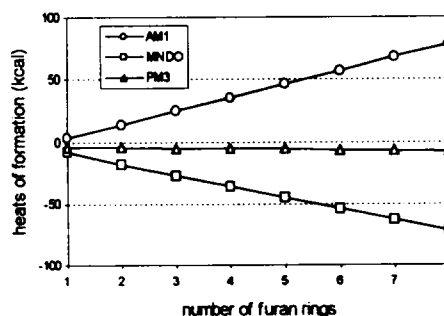


Figure 3. Heats of formation in kcal for all-trans furan oligomers

To get the limiting values of the heat of formation per oligomer subunit, two different ways were used in this study: $\{\text{value}(n)/n\}$ and $\{\text{value}(n) - \text{value}(n-1)\}$, where n is the number of subunits or oligomer rings. These methods are referred to as $/n$ and $/s$, respectively¹¹, and the values are shown in Figure 4 and Figure 5. All the limiting values were almost

constant with the increase of the number of the rings even though there still exists the discrepancy between three different semi-empirical methods. In Figure 4, /n and /s methods gave the same limiting values per subunit by complete convergence using AM1, but not in MNDO and PM3 yet. In Figure 5, only the MNDO gives the same /n and /s converged values.

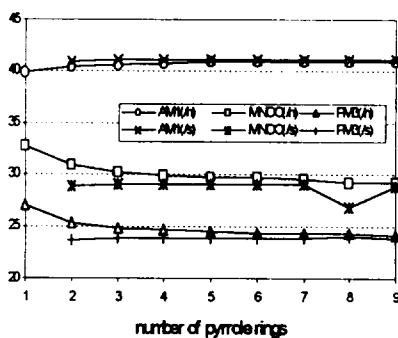


Figure 4. Heats of formation per subunit (referred to as /n and /s) in kcal for all-trans pyrrole oligomers

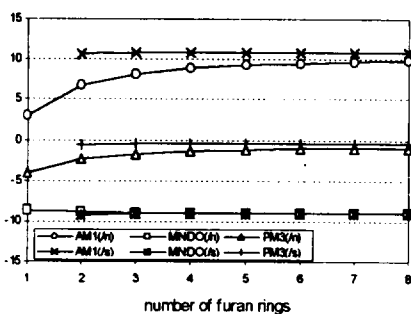


Figure 5. Heats of formation per subunit (referred to as /n and /s) in kcal for all-trans furan oligomers

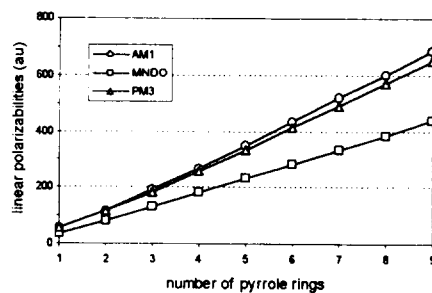


Figure 6. Linear polarizabilities (a.u.) for all-trans pyrrole oligomers

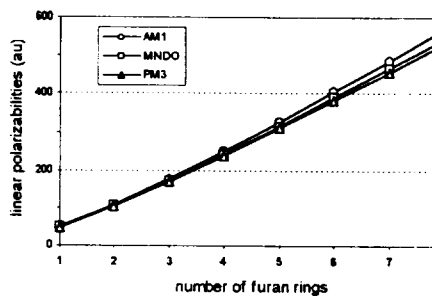


Figure 7. Linear polarizabilities (a.u.) for all-trans furan oligomers

Based on the optimized geometries of all-trans pyrrole and furan oligomers by AM1, MNDO, PM3 approximations, the linear and nonlinear optical properties were calculated using the same approximations with the finite-field method. And the linear polarizabilities are shown in Figure 6 and Figure 7. For the all-trans pyrrole oligomers, the AM1 and PM3 values increase constantly with quite similar rates, but MNDO values increase slower as shown in Figure 6. For the all-trans furan oligomers, as shown in

Figure 7, the AM1, MNDO, PM3 values are increasing with almost same rates.

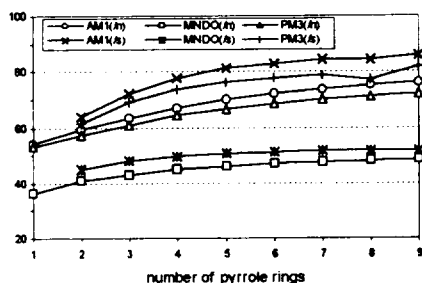


Figure 8. Linear polarizabilities per subunit (referred to as α/n and α/s) in a.u. for all-trans pyrrole oligomers

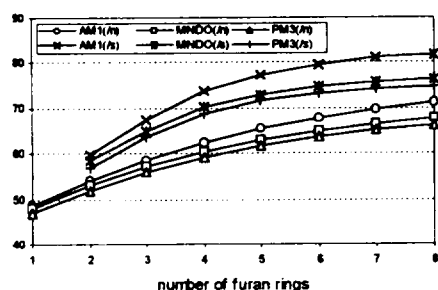


Figure 9. Linear polarizabilities per subunit (referred to as α/n and α/s) in a.u. for all-trans furan oligomers

The limiting subunit values of the linear polarizabilities of these oligomers as referred above are shown in Figure 8 and Figure 9. Up to 9 pyrrole rings and 8 furan rings the limiting α values did not converge, but possible behavior of convergence is expected by increasing the repeating

units. The difference between α/n and α/s limiting α values was about 10 a.u. in both oligomers except in case of pyrrole oligomers by MNDO. Also it can be noted that the α/s values approach faster to the asymptotic limits than the α/n values, indicating α/s method may be more preferable for the convergence procedure.

The second hyperpolarizabilities for all-trans pyrrole oligomers were calculated and the results are shown in Figure 10. Here the AM1 and PM3 methods give fully trans structures after their optimization procedures, so that the maximum delocalization of π electrons can be achieved in this conjugated system, giving high γ values. However, the MNDO optimized geometry of trans pyrrole oligomers was a twisted chain style structure with about 114° dihedral angles between two adjacent pyrrole rings, so that it does not achieve full delocalization of the π electrons. Therefore the γ values from MNDO are much less than those of totally delocalized trans structure from AM1 and PM3. It can be seen from Figure 10 that the γ values from MNDO are 5-7 times smaller than those from PM3 and AM1 in the case of 9 ring system.

The second hyperpolarizabilities for all-trans furan oligomers are shown in Figure 11. In this case, the AM1, MNDO and PM3 semi-empirical methods all give the fully trans optimized structures so that their γ values are in good

agreement one another.

The slightly higher AM1 γ values can be explained from the fact that conformational deviations in bond lengths and angles exist in AM1 as compared to MNDO and PM3 geometries.

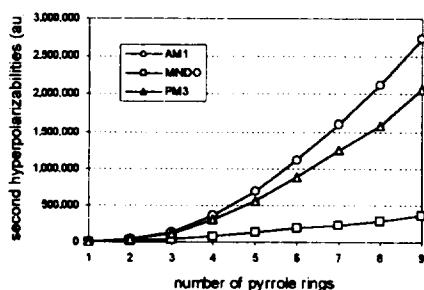


Figure 10. Second hyperpolarizabilities(a.u.) for all-trans pyrrole oligomers

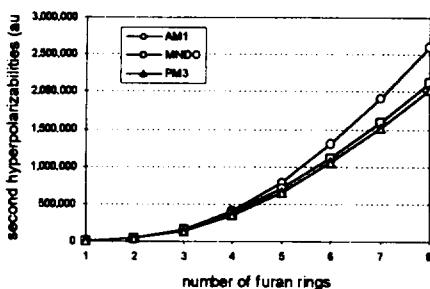


Figure 11. Second hyperpolarizabilities(a.u.) for all-trans furan oligomers

It should also be noted that the γ curves in Figure 10 and 11 start out with a positive curvature but approach linear for large n , indicating a possible prediction of the approximate calculation of γ values at the polymer limit by the computation of a fixed

value per subunit. Such extrapolations had been applied above for the cases of the heats of formation and the linear polarizabilities, and can be used again for the second hyperpolarizabilities, too. To find the limiting γ values per subunit, the extrapolation procedure with logarithms can be applied, where asymptotic limits are assumed as n approaches infinity, that is¹²,

$$\log A(n) = a + \frac{b}{n} + \frac{c}{n^2}$$

where $A(n)$ is the γ value per subunit and a , b , c are the fitting parameters. Thus when n approaches infinity, the extrapolated limiting value is given as $A(n) = 10^a$. The behavior of the limiting γ values per subunit for the all-trans pyrrole and furan oligomers is shown in Figure 12 and 13. It seems from these results that the limiting subunit γ values approach the asymptotic limits, but the convergence is not yet achieved. The predicted limiting subunit γ values for these oligomers are given in Table 1. The $/n$ and $/s$ methods should give the same result at the infinite polymer limit, but $/s$ limiting values are twice the $/n$ results as can be seen in Table 1. This indicates that the second hyperpolarizability of the extended π electron system still has a large contribution from further electron delocalization. It can also be seen from these figures that $/s$ values are converging to the limits faster than $/n$

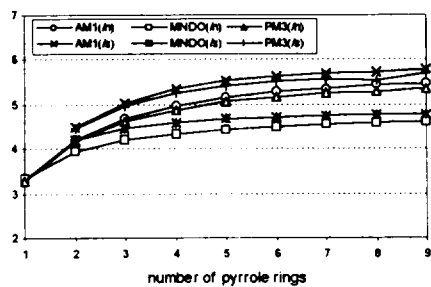


Figure 12. Logarithm of the second hyperpolarizabilities per subunit (referred to as /n and /s) in a.u. for all-trans pyrrole oligomers

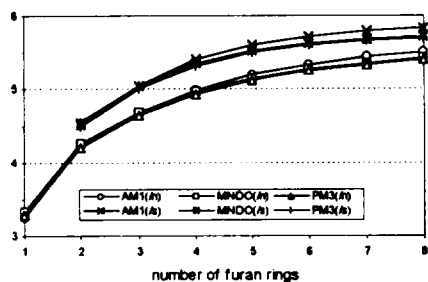


Figure 13. Logarithm of the second hyperpolarizabilities per subunit (referred to as /n and /s) in a.u. for all-trans furan oligomers

values, indicating /s is preferable to /n at moderate oligomer sizes. Increasing the number of subunits included in the calculations should reduce the difference between /n and /s methods and give the same converged limiting value. The discrepancies between semi-empirical results may again be explained as mainly due to the differences in

predicted optimized geometries.

Table 1. Predicted limiting values in 10^5 a.u. for the second hyperpolarizabilities of all-trans 9 ring pyrrole and 8 ring furan oligomers

	pyrrole oligomer		furan oligomer	
	/n	/s	/n	/s
AM1	3.03	5.96	3.25	6.84
MNDO	0.39	0.59	2.65	5.26
PM3	2.29	4.79	2.53	5.05

Conclusion

The primary goal in this work was to calculate the second hyperpolarizabilities of pyrrole and furan oligomers which have long conjugation chains and fully extended π electron delocalizations so that the large γ values would be expected. The methods used in this study were AM1, MNDO, and PM3 semi-empirical MO approximations in which the finite-field method was implied for a static external electric field. The calculation results were compared among three different semi-empirical methods so that the molecular structures could be investigated and related with the corresponding γ behaviors. It would be more meaningful if these semi-empirical predictions could be compared with the available experimental results even though there would exist several experimental factors which make a direct comparison more difficult. And it should be mentioned that the

experimental values are frequency dependent but all the results reported here are at static electric fields, so that the direct comparison can not be made. Also the purpose was put to achieve a limiting γ value per subunit so that the nonlinear optical behavior of various interesting polymers would be predicted without direct calculations. The /n and /s methods were used to predict the limiting γ values per subunit, and it was shown that /s converged faster than /n to the asymptotic limit. Up to 9 rings of the oligomers considered in this work the satisfactory convergence for the limiting values was not achieved, because the calculations have not been done for large enough polymer units. However the patterns approaching to an asymptotic limit could be seen quite nicely, so it is expected that the convergence would reach if more ring sizes are included in the calculations. It is hoped that the nonlinear optical behaviors for other interesting heterocyclic compounds are to be calculated and investigated further in future. Finally it is hoped that the nonlinear optical property calculations will be improved with modifications such as atomic correction factors, vibrational effects, and frequency dependence.

References

1. Prasad, P. N. and Williams, D. J., *Introduction to Nonlinear Optical Effects in Organic Molecules and Polymers*, Wiley Interscience, New York, 1991.
2. Shen, Y. R., *The Principles of Nonlinear Optics*, Wiley and Sons, New York, 1984.
3. Baldwin, G. C., *An Introduction to Nonlinear Optics*, Plenum Press, New York, 1969.
4. Chemla, D. S. and Zyss, J., *Nonlinear Optical Properties of Organic Molecules and Crystals*, Vol. 1 and 2, Academic Press, Orlando, 1987.
5. Cohen, H. D. and Roothaan, C. C. J., *J. Chem. Phys.*, **43**, S34, 1965.
6. Buckingham, A. D. and Orr, B. J., *Q. Rev. Chem. Soc.*, **21**, 195, 1967.
7. Bartlett, R. J. and Purvis, G. D., *Phys. Rev. A.*, **20**, 1313, 1979.
8. Kim, W. H., *Semi-empirical Calculations of Nonlinear Optical Properties of Organic Molecules and Polymers*, Univ. of Memphis, 1991.
9. Coolidge, M. B. and Stewart, J. J. P., *MOPAC MANUAL V6.0*, QCPE, 1990.
10. (a) Dewar, M. J. S., Zoebisch, E. G., Healy, E. F. and Stewart, J. J. P., *J. Am. Chem. Soc.*, **107**, 3902, 1985. (b) Dewar, M. J. S. and Thiel, W., *J. Am. Chem. Soc.*, **99**, 4899, 1977. (c) Stewart, J. J. P., *J. Comp. Chem.*, **10**, 209, 221, 1989.
11. Kurtz, H. A., *Int. J. Quant. Chem.: Quant. Chem. Symp.*, **24**, 791, 1990.
12. Hurst, G. J. B., Dupuis, M. and

Clementi, E., J. Chem. Phys., **89**, 385, 1988.

[국문초록]

본 연구에서는 AM1, MNDO, PM3의 반경험적 계산방법을 사용하여 pyrrole 중합체와 furan 중합체의 all-trans 구조를 최적화하였으며, 이로부터 유한장 방법과 함께 이들 중합체에 대한 이차초편극도 계산을 수행하였다. 이 중합체들의 π 전자들이 최대로 비편재화되어 있을 때 큰 이차초편극도값이 얻어졌

다. 또한 이차초편극도의 증가는 이 중합체의 공액 길이에 직접적으로 비례하였다. 중합체의 구성단위당 한계 이차초편극도값이 /n방법과 /s방법에 의해 계산되었으며, /s방법이 /n방법보다 극한값에 더 빨리 수렴함을 보였다. 본 연구에서 다루어진 구성단위가 9개까지인 중합체의 경우, /s방법에 의한 한계 이차초편극도는 /n방법에 의한 한계 이차초편극도의 2배였으며, 중합체 구성단위의 길이를 무한개로 연장할 경우 두 방법에 의한 한계 이차초편극도는 같아질 것이다.